

UC Riverside

UC Riverside Previously Published Works

Title

Cell and Protein Recognition at a Supported Bilayer Interface via In Situ Cavitand-Mediated Functional Polymer Growth

Permalink

<https://escholarship.org/uc/item/3kh9v5bc>

Journal

Langmuir, 31(41)

ISSN

0743-7463

Authors

Perez, Lizeth
Ghang, Yoo-Jin
Williams, Preston B
[et al.](#)

Publication Date

2015-10-20

DOI

10.1021/acs.langmuir.5b03124

Peer reviewed



Published in final edited form as:

Langmuir. 2015 October 20; 31(41): 11152–11157. doi:10.1021/acs.langmuir.5b03124.

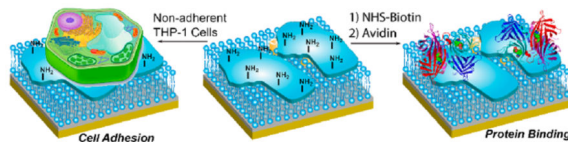
Cell and Protein Recognition at a Supported Bilayer Interface via In Situ Cavitand-Mediated Functional Polymer Growth

Lizeth Perez, Yoo-Jin Ghang, Preston B. Williams, Yinsheng Wang, Quan Cheng, and Richard J. Hooley*

Department of Chemistry, University of California—Riverside, Riverside, California 92521, United States

Abstract

Water-soluble deep cavitands embedded in a supported lipid bilayer are capable of anchoring ATRP initiator molecules for the in situ synthesis of primary amine-containing polymethacrylate patches at the water:membrane interface. These polymers can be derivatized in situ to incorporate fluorescent reporters, allow selective protein recognition, and can be applied to the immobilization of nonadherent cells at the bilayer interface.



INTRODUCTION

A variety of different species are displayed at the mammalian cell membrane surface, ranging from small molecule epitopes to biomacromolecules and glycopolymers.¹ These species are vital for controlling cellular function and response, and so they provide enticing targets for further study.² The complexity of the cell membrane surface has led to the application of supported lipid bilayers as controlled mimics of the interface.^{3,4} Many biorelevant targets such as proteins,⁵ nucleotides,⁶ small molecules,⁷ glycopeptides,^{8,9} glycopolymers^{10–12} or even whole living cells¹³ can be incorporated into supported lipid bilayers, often exploiting covalent modifications such as lipidation for attachment. As the targets become larger, the synthetic challenges associated with covalent lipidation increase, especially in the solubility and purification of large biomolecules.⁵ A recognition system that can be created in situ at a bilayer interface and be tailored for the immobilization of biorelevant targets would solve a number of these problems and allow the simple creation of

*Corresponding Author. University of California Riverside, Department of Chemistry, Riverside, CA, 92521. richard.hooley@ucr.edu.

ASSOCIATED CONTENT

Supporting Information

The Supporting Information is available free of charge on the ACS Publications website at DOI: 10.1021/acs.langmuir.5b03124. Characterization and SPR sensorgrams not in the text (PDF)

Notes

The authors declare no competing financial interest.

complex cell surface mimics. Of course, this goal requires reactive functionality to be displayed at a bilayer membrane. This requires the use of bioorthogonally reactive species that are tolerant to the bilayer environment, and few examples are known.¹⁴ In addition to the challenges associated with in situ reactivity at bilayer interfaces, macromolecular recognition often requires a large surface area for good affinity. Cells employ polymeric species such as glycans for target recognition, and there are examples of synthetic polymers being applied for this purpose in cellular^{15–17} or synthetic membrane environments.^{18–20} These polymers are preformed before addition, however, and many polymer types are limited by their insolubility in aqueous solution.

An alternative to the chemical synthesis and derivatization of functional polymers before introduction to a bilayer membrane is to perform the polymerization in situ. The polymerization must be compatible with the bilayer environment, allowing successful, robust reaction while maintaining the integrity of the membrane. Further derivatization of this polymer surface at the bilayer interface also requires the presence of biorthogonal, reactive functional groups in the monomer, complicating the polymerization process.

EXPERIMENTAL SECTION

Calcinated Chip Preparation

Gold substrates were fabricated with a 2 nm thick chromium adhesion layer, followed by the deposition of a 46 nm thick gold layer via e-beam evaporation on cleaned glass slides. The nanoglassified layers were constructed on the surface based on a previous layer-by-layer protocol.²⁴

Fabrication of Cavitand: Supported Lipid Bilayer

The calcinated gold substrate was first rinsed with ethanol and nanopure water and after drying under gentle stream of nitrogen gas was then clamped down by a flow cell on a high-refractive index prism for SPR measurement. POPC vesicles (1 mg/mL, see Supporting Information for construction method) in 10 mM PBS (150 mM NaCl, pH 7.4) were injected through a flow-injection system and incubated for 15 min to allow vesicle fusion on the hydrophilic calcinated gold surface, forming a smooth bilayer membrane. After 5 min of rinsing to remove excess vesicles from the surface, 0.7 mg/mL cavitand **1** in 10% DMSO solution was subsequently injected and incubated for 20 min. The surface was extensively rinsed with water, followed by incubation with 10 mg/mL initiator **2** in aqueous solution for 5 min. After 5 min of rinsing to remove unbound initiator **2** from bilayer lipid membrane, atom transfer radical polymerization (ATRP) reaction was initiated by the injection of monomer **3–4** (0.7 M HEMA **3**, and 0.7 M AEMA **4**) and catalyst (15 mM CuBr/30 mM 2,2'-bipyridine/22 mM L-ascorbic acid or 15 mM FeCl₂/30 mM 1,10-phenanthroline/22 mM L-ascorbic acid in a 1:2:1.5 molar ratio) mixture solution. After 20 min of incubation for polymer growth, ATRP reaction was terminated by 5 min rinsing with water.

In Situ Reactions of Poly(AEMA)

After poly(AEMA) formation on the lipid membrane surface, NHS-biotin was injected into the SPR flow cell (1 mg/mL in 10% DMSO aqueous solution) and incubated for 20 min

followed by 5 min rinsing. Avidin (1 mg/mL in 10 mM PBS) was then injected, incubated for 20 min, and washed for 5 min. The reaction with NBD-Cl followed the same procedure.

Cell Sample Preparation

Human monocytic THP-1 cells (ATCC TIB-202) were cultured at 37 °C and 5% CO₂ in RPMI 1640 media supplemented with 10% FBS, 100 U/ml penicillin, 100 µg/mL streptomycin, and 50 µM 2-mercaptoethanol. Cells were harvested by centrifugation and washed three times with ice cold deionized H₂O. Immediately after washing, cells were resuspended in ice cold deionized H₂O to a final concentration of 7.5×10^6 cells/mL.

Cellular Adhesion Studies

After poly(AEMA) formation, human monocytic THP-1 cells were injected into the SPR flow cell and incubated for 20 min, then rinsed for 5 min with nanopure water. The gold chip was then removed from the SPR system and covered with a microscope coverslip and visualized under an optical microscope.

RESULTS AND DISCUSSION

We have previously described a synthetic molecular recognition based system that allows controlled polymer growth at a supported bilayer interface by noncovalent recognition and display of a suitable atom transfer radical polymerization (ATRP)^{21,22} initiator by a water-soluble host molecule embedded in the membrane.²³ Deep cavitands such as **1** (Figure 1) are lipophilic, and can incorporate in lipid bilayers while retaining their host abilities.^{24–27} The most strongly binding guests for cavitands such as **1** are trimethylammonium species such as acetylcholine.²⁸ These targets are bound in competitive environments by exploiting cation– π interactions between the faces of the aromatic cavitand walls and the soft cationic guest.²⁹ Choline-derived ATRP initiator **2** is a strongly binding guest for cavitand **1**, and can be presented to the bilayer surface by simple injection. Subsequent injection of a suitable monomer (e.g., hydroxyethyl methacrylate HEMA **3**) and CuBr•bipy as catalyst allowed the growth of a polymeric surface at the bilayer interface, held in place by multiple noncovalent contacts between the initiator termini and cavitands embedded in the bilayer.²³ The ATRP process is tolerant to aqueous media and can be performed under very mild conditions that maintain the fluid membrane below the polymer patches.

Our initial efforts to grow polymers at the bilayer interface established the feasibility of the process, but polymerization of functionalized monomers was generally unsuccessful.²³ Whereas simple unfunctionalized monomers such as HEMA and methyl methacrylate (MMA) gave controllable polymer growth at the interface, larger monomers suffered from insolubility problems in buffered aqueous solution. Highly water-soluble saccharide-linked methacrylates showed weaker affinity for the cavitands in the bilayer and are easily washed from the surface. The obvious solution would be to perform a second reaction on the freshly formed polymer, as there are myriad ways to postsynthetically derivatize poly(HEMA).²¹ Unfortunately, none of those methods work in aqueous solution, so we sought to introduce an orthogonal reactive functional group to the polymer surface. The simplest group is a primary amine, the central functionality used in surface and biomolecule derivatization.

Amines are capable of nucleophilic reactivity in water, and a wide variety of reactions are possible.¹⁴ The challenge, however, is that primary amines are uniquely unsuited to ATRP, as they show strong coordination to metal ions, leaching the catalyst from the reaction mixture and causing low turnovers, poor polydispersities, and the formation of somewhat random polymer sizes.^{21,22} Fortunately, narrow polydispersities are unimportant for our goals. A small, reactive polymer patch is perfectly sufficient to allow in situ reactivity at the bilayer, and so we investigated the polymerization of AEMA **4** at a bilayer interface.

The supported lipid bilayer was generated by established methods, and the experimental setup is illustrated in Figure 2.²⁴

The surface was prepared by a layer-by-layer calcination procedure involving the formation of a mercaptopropionic acid (MPA) self-assembled monolayer on a clean gold surface followed by six layers of sodium silicate (22 mg/mL, pH 9.5) and polyallylamine HCl (avg. MW 17,500, pH 8). Calcination at 450 °C forms a silica nanolayer at the interface, enabling lipid adhesion. The gold chips were attached to a flow cell setup with a dual channel injection capability, allowing real time, noninvasive monitoring of adhesion processes by Surface Plasmon Resonance (SPR) spectroscopy.³⁰ Preformed POPC (palmitoyl-oleyl phosphocholine) bilayer vesicles were injected into the flow cell and exposed to the surface, forming a fluid supported lipid bilayer. Water-soluble tetracarboxylate cavitand **1** can be injected to this bilayer and self-incorporate into the upper leaflet.²⁴ This exposes its open cavity to the exterior milieu, and an SPR sensorgram of the process is shown in Figure 3b. After insertion of cavitand (0.7 mg/mL, 10% DMSO:H₂O) into the supported lipid bilayer, a robust 0.20° change in resonance angle θ is observed after washing away the injection solvent (and any unincorporated **1**). The SPR response is qualitatively related to the amount of incorporated cavitand, and a 0.20 ± 0.04° response change can be consistently achieved. Increased [**1**] (up to 2 mg/mL) does not change the response, indicating saturation in the incorporation of **1**. The cavitand remains in the bilayer during the washing phase, and no cavitand can be detected by MS analysis of the washings.²⁶ The ATRP initiator molecule **2** can be bound via shape-fitting noncovalent interactions with the membrane-bound cavities upon simple injection into the flow cell. This small guest causes only a slight change in resonance angle, consistent with that of other similarly sized guests.^{23,24} The initiator is mildly reactive to water, so polymerization is performed within 5 min of injection.

As primary amines are poor substrates for ATRP, we initially optimized the catalyst system (Figure 3 and Supporting Information). Combinations of three ligands (2,2 bipyridyl (bipy), 9,10-phenanthroline (phen) and tris(benzimidazole)-triethyleneamine (tbte)) and two metal salts (FeCl₂ and CuBr) in the presence of ascorbic acid as reductant were tested for ATRP effectiveness.²¹ Phen and bipy are bidentate and more weakly coordinating, whereas tbte can occupy up to 4 sites on the metal center, potentially limiting AEMA coordination and catalyst inactivation. The polymerization was performed by simple injection of a 0.7 M solution of monomer AEMA **4** and 15 mM catalyst complex (1:2 ligand: metal ratio) in 10 mM phosphate buffered saline (PBS), and the relative amount of polymerization monitored by resonance angle change after washing by SPR. Interestingly, the more tightly coordinated CuBr•phen and CuBr•tbte complexes gave less effective polymer formation ($\theta = 0.09^\circ$ (Figure 3b) and 0.14° (see Supporting Information), respectively) than CuBr•bipy ($\theta =$

0.20° (Figure 3c)). FeCl₂ was equally effective as catalyst metal (see Supporting Information), which can be beneficial for any application of this method in biological systems due to the lower toxicity of Fe (II). The FeCl₂-phen catalyst was most effective, providing consistent responses of $\Delta\theta = 0.20^\circ$, although there was a smaller variation between different ligands in this case.

Further variables were tested in the optimization process. As might be expected, variation of monomer concentration does not greatly affect the size of poly(AEMA) formed. A 0.7 M solution contains a large excess of monomer with respect to bound initiator, and the 0.20° resonance angle change indicates a polymer size similar to that of the POPC bilayer itself. The AEMA concentration was varied in increments from 0.7 M to 1.4M, but no appreciable difference in resonance angle was observed upon polymerization. The standard incubation time was 20 min. Incubation times longer than this (60 or 90 min) did not show any appreciable increase in polymerization at the surface. This suggests relatively rapid catalyst inactivation, as is to be expected from the coordinating and reducing nature of AEMA. In addition, increasing the initiator **2** concentration did not increase the polymer size. While determining the exact concentration of cavitand **1** absorbed in the membrane is challenging, studies with vesicles preloaded with cavitand suggest that a 2% cavitand loading gives a similar amount of guest recognition.²⁷ The dissociation constant of R-NMe₃⁺-based guests for cavitand **1** in a POPC bilayer is on the order of micromolar,²⁶ indicating that the host is most likely saturated with initiator before ATRP. Finally, the living nature of the polymerization was tested. ATRP is a living polymerization process, allowing further polymerization upon injection of additional monomer and catalyst to the reaction. We previously showed that the ATRP of HEMA **3** displayed living characteristics at the bilayer interface,²³ and polymer growth could be extended multiple times by monomer injections. This is not the case for AEMA **4**: after initial polymerization, subsequent injections of **4** and catalyst mixture gave no observable increase in resonance angle upon SPR analysis (see Supporting Information for sensorgrams). Not only do the amine groups inactivate the catalyst mixture after reaction, they evidently also terminate the process, limiting further reaction at the interface.

This inactivation process limits the polymerization to the formation of small microscale polymer patches. The polymerization occurs consistently, but there is variation in SPR response ($\delta(\Delta\theta) = \pm 0.04^\circ$) and therefore polymer size between individual runs. While the small size of the polymers may limit their use in solution environments, the thin polymer layer is perfectly suited for further derivatization at the bilayer interface. No disruption of the membrane is seen, and the polymer patches display multiple primary amine groups at the surface. To establish their functionality, we initially explored a simple in situ reaction with fluorescent dye 4-chloro-7-nitrobenzofurazan (NBD-Cl). This process has the added advantage of providing an alternate method of polymer characterization other than SPR, something that is quite challenging. The polymer patches cannot be removed from the surface by simple washing to allow isolation and postsynthetic characterization, nor are surface analysis techniques such as XPS or IR spectroscopy applicable to the complex lipid bilayer environment. The bilayer can be stripped from the surface along with polymer and cavitands, but the presence of the charged POPC lipids renders MS analysis useless.

Confocal microscopy of the fluorescent surface after reaction with NBD-Cl allows some quantitation of patch size, as shown in Figure 3d,e. After poly(AEMA) formation, a 1 mg/mL aqueous solution of NBD-Cl was injected into the flow cell and incubated for 20 min. After washing, a small resonance angle change was observed, consistent with surface reaction between poly(AEMA) and the low M_w NBD-Cl. The chip was imaged using confocal microscopy, and the presence of individual patches of fluorescence atop the bilayer are clearly seen, indicating derivatization of the poly(AEMA) surface. These patches vary in size and provide a partial coating of the bilayer interface, with no disruption of the membrane itself. It is notable that the ATRP of AEMA appears to form discrete, micrometer-sized polymer patches atop the bilayer, as cavitand **1** is fluid in the membrane, and displays a lateral diffusion similar to that of POPC lipids.²⁴ While the polyAEMA shows incomplete surface coverage, the process is quite variable, and different coverages are observed with different runs. Full, consistent surface coverage can be obtained by polymerization of polyHEMA or polyMMA (see below).²³ The small size of the polyAEMA patches, and their variability in size from experiment to experiment are consistent with inefficient, monomer-terminated ATRP. It is also possible that the reaction with the water-sensitive NBD-Cl does not occur at full conversion, although a large excess was used for testing. NBD-Cl is poorly water-soluble, and could lead to localized reaction at the interface: the SPR analysis of polyAEMA formation is far more consistent than the visualization, and so the size of the patches may be quite variable, although they do form consistently.

Even though the size of the polymers is somewhat variable, their synthesis is consistent, and they are capable of in situ reactions at the membrane surface. The next question is whether these functional polymer coatings are amenable to other, more challenging in situ reactions. As can be seen in Figure 4, the surfaces are also capable of both epitope display and subsequent protein recognition. The poly(AEMA) surface was derivatized with biotin groups by injection of the *N*-hydroxysuccinimide (NHS) active ester of biotin atop the surface (Figure 4b). As was seen with the NBD-Cl reaction, a small resonance angle change was observed upon injection of NHS-biotin into the SPR flow cell. After washing away the unattached excess of reactant and injection of avidin, a larger ($\theta = 0.35^\circ$) response was observed, indicating immobilization of the much larger avidin protein at the surface. The protein recognition process only occurs upon display of biotin at the polymer surface: if the reaction is repeated with underivatized biotin (Figure 4c), no avidin adhesion is observed. Biotin has no affinity for the poly(AEMA) surface under the buffered conditions used for the injection, and is easily washed away. In addition, there are also no charge-based interactions between avidin and the cationic polymer surface. Only specific biotin:avidin interactions allow immobilization of the protein at the bilayer interface, providing selective biorecognition via the cavitand-mediated polymer synthesis.

The poly(AEMA) surface can be exploited in multiple ways: besides the core nucleophilicity of the displayed amine groups, the resting state of the polymer under the pH 7.4 buffered conditions is also cationic. This suggests a capability to recognize even larger species such as living cells. While eukaryotic cells have little to no affinity for hydrophilic surfaces or POPC bilayers,¹³ cationic graft copolymers are well-known to attach to living

cells and mediate target transport.¹⁴ Even though the bilayer is somewhat fragile, the thin layer of polymer at the bilayer is a suitable protecting agent, and should be able to act as the “glue” required for cell adhesion between the bilayer and living cells. The cell recognition properties of the POPC:1:2:poly(AEMA) construct were tested using human monocytic THP-1 cells, which are nonadherent. THP-1 cells were grown in RPMI growth medium, then centrifuged to form a pellet, and the high salt concentration medium removed. The cells were then rinsed with 10 mM PBS buffer before being suspended in either 10 mM PBS buffer or pure deionized water to a cell density of 7.5×10^6 cells/mL just before injection into the relevant flow cell environment.

Three different surfaces were tested to illustrate the function and selectivity of the cationic poly(AEMA) surface: a pristine POPC bilayer, neutral, hydrophilic poly(HEMA) (grown at the surface via cavitand-mediated initiator display as previously reported²³), and freshly grown poly(AEMA). As would be expected, injection of THP-1 cells showed a minimal response at the pristine POPC bilayer interface. After washing, the chip was removed from the flow cell (without removal of the aqueous environment around the bilayer, which could cause defects in the fragile SLB) and analyzed by visible light microscopy. Some small defects were seen (Figure 5a), but very few cells adhered to the bilayer, and the small number that did were most probably attached to the silica surface rather than the bilayer.²³ Similarly, no cell adhesion was seen with the hydrophilic, neutral poly(HEMA) surface. As described above, polymerization of HEMA **3** is more efficient than that of AEMA, and a thicker, more complete coating is formed that displays no affinity for the nonadherent THP-1 cells (Figure 5b). The SPR sensorgram showed no resonance angle change upon cell addition, and no cells were visible at the surface via microscopy.

The poly(AEMA) surface, however, was fully functional and was able to immobilize the cells, as predicted. After introduction and incubation of THP-1 cells to the freshly grown poly(AEMA) surface, a substantial, retained resonance angle change was observed, indicating immobilization of cells at the cationic polymer interface. Visualization of the chip after removal from the flow cell confirmed the attachment of cells on the surface by poly(AEMA) (Figure 5c). The cells are smaller than the visualized polymer patches from Figure 3e, and are spaced randomly atop the bilayer (see Supporting Information). The process was repeatable, although the display pattern was somewhat variable, consistent with the uncontrolled polymer growth process. The cell attachment process proved robust, as the cells were not removed from the surface even after many minutes of washing in the flowcell with PBS buffer. The injection medium was unimportant, as the cells remained adhered either in pure water or higher ionic strength buffer. THP-1 cells are quite small, and the polymer patches are large enough to provide a cationic surface area sufficient to allow adhesion of the cells.

CONCLUSIONS

Here, we have shown that membrane-embedded deep cavitands are capable of promoting the polymerization of primary amine containing monomers at a supported bilayer interface, allowing functionalized polymers to be formed in a controllable and repeatable manner. The amine functions limit excessive, uncontrolled polymerization and favor the formation of

micrometer sized discrete “archipelagos” of poly(AEMA) at the water: bilayer interface. These polymer patches can be reacted in situ to allow display of fluorescent reporters or epitopes for protein immobilization, as well as acting as “molecular glue” by displaying a cationic surface for the soft immobilization of nonadherent cells at the bilayer. The use of nontoxic ATRP catalysts and the simple experimental procedure indicates that this method of in situ reactivity will have applications in cell surface engineering and the controlled creation of complex cell surface mimics.

Supplementary Material

Refer to Web version on PubMed Central for supplementary material.

ACKNOWLEDGMENTS

The authors would like to thank the National Science Foundation (CHE-1151773 to R.J.H., CHE-1413449 to Q.C.), the UC Cancer Research Coordinating Committee, and the National Institutes of Health (R01 ES019873 to Y.W.), L.P. and P.B.W. acknowledge support through a U.S. Department of Education GAANN Award #P200A120170.

REFERENCES

1. Triola G, Waldmann H, Hedberg C. Chemical Biology of Lipidated Proteins. *ACS Chem. Biol.* 2012; 7:87–99. [PubMed: 22148864]
2. Hymel D, Peterson BR. Synthetic cell surface receptors for delivery of therapeutics and probes. *Adv. Drug Delivery Rev.* 2012; 64:797–810.
3. Castellana ET, Cremer PS. Solid supported lipid bilayers: From biophysical studies to sensor design. *Surf. Sci. Rep.* 2006; 61:429–444.
4. Groves JT, Boxer SG. Micropattern formation in supported lipid membranes. *Acc. Chem. Res.* 2002; 35:149–157. [PubMed: 11900518]
5. Brunsveld L, Kuhlmann K, Alexandrov K, Wittinghofer A, Goody RG, Waldmann H. Lipidated Ras and Rab peptides and proteins - synthesis, structure, and function. *Angew. Chem., Int. Ed.* 2006; 45:6622–6646.
6. Zope HR, Versluis F, Ordas A, Voskuhl J, Spaik HP, Kros A. In Vitro and In Vivo Supramolecular Modification of Biomembranes Using a Lipidated Coiled-Coil Motif. *Angew. Chem., Int. Ed.* 2013; 52:14247–14251.
7. Boonyarattanakalin S, Martin SE, Dykstra SA, Peterson BR. Synthetic Mimics of Small Mammalian Cell Surface Receptors. *J. Am. Chem. Soc.* 2004; 126:16379–16386. [PubMed: 15600339]
8. Godula K, Rabuka D, Nam KT, Bertozzi CR. Synthesis and Microcontact Printing of Dual End-Functionalized Mucin-like Glycopolymers for Microarray Applications. *Angew. Chem., Int. Ed.* 2009; 48:4973–4976.
9. Krishnamurthy VR, Wilson JT, Cui W, Song X, Lasanajak Y, Cummings RD, Chaikof EL. Chemoselective Immobilization of Peptides on Abiotic and Cell Surfaces at Controlled Densities. *Langmuir.* 2010; 26:7675–7678. [PubMed: 20450194]
10. Rabuka D, Forstner MB, Groves JT, Bertozzi CR. Noncovalent Cell Surface Engineering: Incorporation of Bioactive Synthetic Glycopolymers into Cellular Membranes. *J. Am. Chem. Soc.* 2008; 130:5947–5953. [PubMed: 18402449]
11. Godula K, Umbel ML, Rabuka D, Botyanszki Z, Bertozzi CR, Parthasarathy R. Control of the Molecular Orientation of Membrane-Anchored Biomimetic Glycopolymers. *J. Am. Chem. Soc.* 2009; 131:10263–10268. [PubMed: 19580278]
12. Harland CW, Botyanszki Z, Rabuka D, Bertozzi CR, Parthasarathy R. Synthetic Trehalose Glycolipids Confer Desiccation Resistance to Supported Lipid Monolayers. *Langmuir.* 2009; 25:5193–5198. [PubMed: 19323499]

13. Groves JT, Mahal LK, Bertozzi CR. Control of Cell Adhesion and Growth with Micropatterned Supported Lipid Membranes. *Langmuir*. 2001; 17:5129–5133.
14. Sletten EM, Bertozzi CR. Bioorthogonal chemistry: fishing for selectivity in a sea of functionality. *Angew. Chem., Int. Ed.* 2009; 48:6974–6998.
15. Wilson JT, Krishnamurthy VR, Cui W, Qu Z, Chaikof EL. Noncovalent Cell Surface Engineering with Cationic Graft Copolymers. *J. Am. Chem. Soc.* 2009; 131:18228–18229. [PubMed: 19961173]
16. Kozlovskaya V, Zavgorodnya O, Chen Y, Ellis K, Tse HM, Cui W, Thompson JA, Kharlampieva E. Ultrathin Polymeric Coatings Based on Hydrogen-Bonded Polyphenol for Protection of Pancreatic Islet Cells. *Adv. Funct. Mater.* 2012; 22:3389–3398. [PubMed: 23538331]
17. Niikura K, Nambara K, Okajima T, Kamitani R, Aoki S, Matsuo Y, Ijro K. Artificial polymeric receptors on the cell surface promote the efficient cellular uptake of quantum dots. *Org. Biomol. Chem.* 2011; 9:5787–5792. [PubMed: 21738911]
18. Hubert DHW, Jung M, German AL. Vesicle Templating. *Adv. Mater.* 2000; 12:1291–1294.
19. Fukuda H, Diem T, Stefely J, Kezdy FJ, Regen SL. Polymer-encased vesicles derived from dioctadecyldimethylammonium methacrylate. *J. Am. Chem. Soc.* 1986; 108:2321–2327. [PubMed: 22175577]
20. Jayasuriya N, Bosak S, Regen SL. Supramolecular surfactants: polymerized bolaphiles exhibiting extraordinarily high membrane-disrupting activity. *J. Am. Chem. Soc.* 1990; 112:5851–5854.
21. Ouchi M, Terashima T, Sawamoto M. Transition Metal-Catalyzed Living Radical Polymerization: Toward Perfection in Catalysis and Precision Polymer Synthesis. *Chem. Rev.* 2009; 109:4963–5050. [PubMed: 19788190]
22. Matyjaszewski K, Tsarevsky NV. Nanostructured functional materials prepared by atom transfer radical polymerization. *Nat. Chem.* 2009; 1:276–288. [PubMed: 21378870]
23. Liu Y, Young MC, Moshe O, Cheng Q, Hooley RJ. A Membrane-Bound Synthetic Receptor Promotes Growth of a Polymeric Coating at the Bilayer-Water Interface. *Angew. Chem., Int. Ed.* 2012; 51:7748–7751.
24. Liu Y, Liao P, Cheng Q, Hooley RJ. Non-Covalent Molecular Recognition of Proteins at a Bilayer Interface by Self-Folding Synthetic Receptors. *J. Am. Chem. Soc.* 2010; 132:10383–10390. [PubMed: 20617792]
25. Ghang Y-J, Schramm MP, Zhang F, Acey RA, David CN, Wilson EH, Wang Y, Cheng Q, Hooley RJ. Selective Cavitand-Mediated Endocytosis of Targeted Imaging Agents into Live Cells. *J. Am. Chem. Soc.* 2013; 135:7090–7093. [PubMed: 23621383]
26. Ghang Y-J, Perez L, Morgan MA, Si F, Hamdy OM, Beecher CN, Larive CK, Julian RR, Zhong W, Cheng Q, Hooley RJ. Anionic Deep Cavitands Enable the Adhesion of Unmodified Proteins at a Membrane Bilayer. *Soft Matter*. 2014; 10:9651–9656. [PubMed: 25366572]
27. Ghang Y-J, Lloyd JJ, Moehlig MP, Arguelles JK, Mettry M, Zhang X, Julian RR, Cheng Q, Hooley RJ. Labeled Protein Recognition at a Membrane Bilayer Interface by Embedded Synthetic Receptors. *Langmuir*. 2014; 30:10161–10166. [PubMed: 25130415]
28. Hof F, Trembleau L, Ullrich EC, Rebek J Jr. Acetylcholine Recognition by a Deep, Biomimetic Pocket. *Angew. Chem., Int. Ed.* 2003; 42:3150–3153.
29. Biros SM, Ullrich EC, Hof F, Trembleau L, Rebek J Jr. Kinetically Stable Complexes in Water: The Role of Hydration and Hydrophobicity. *J. Am. Chem. Soc.* 2004; 126:2870–2876. [PubMed: 14995204]
30. Homola J. Surface Plasmon Resonance Sensors for Detection of Chemical and Biological Species. *Chem. Rev.* 2008; 108:462–493. [PubMed: 18229953]

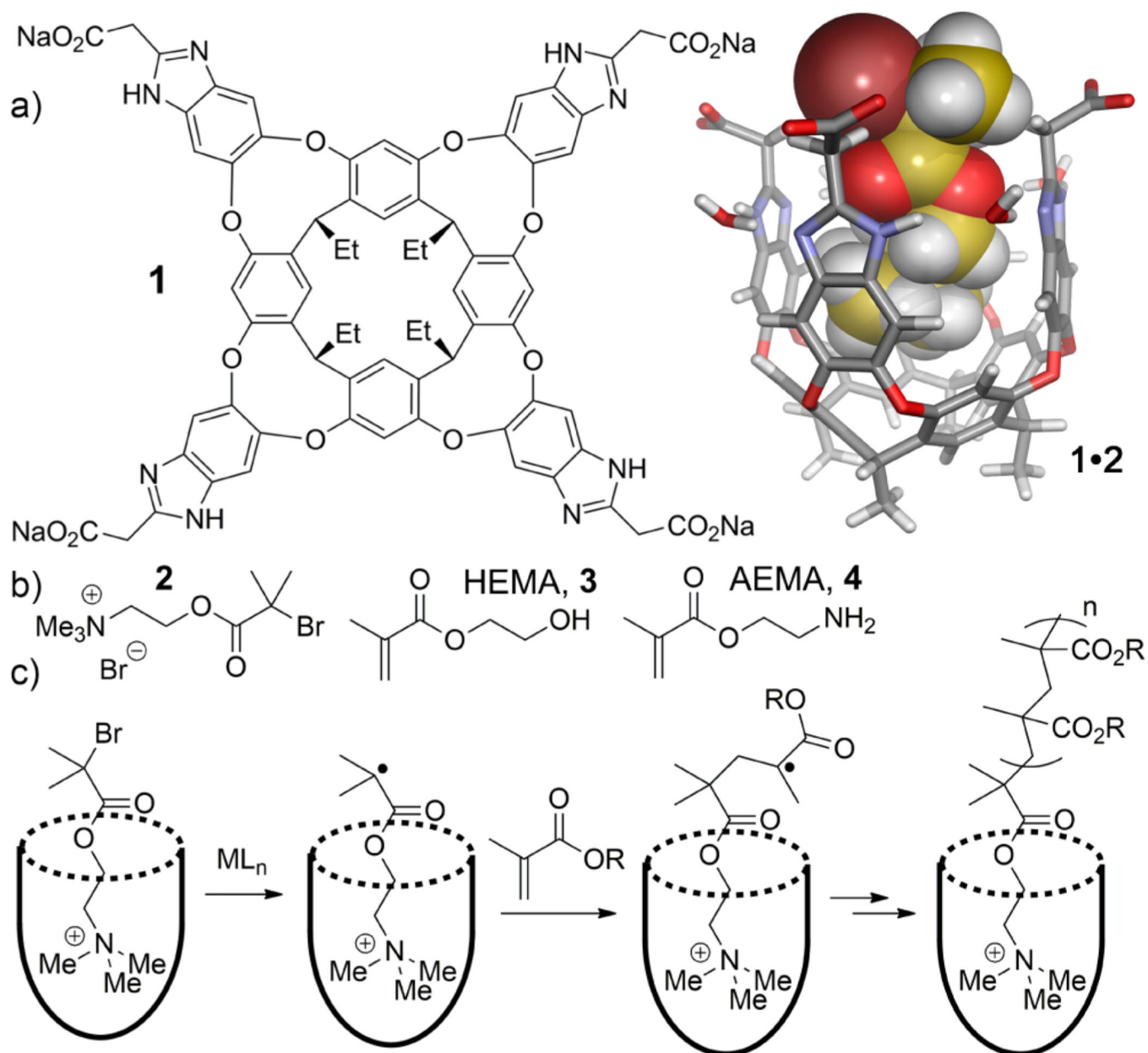


Figure 1.

(a) Water-soluble deep cavitand **1** and the minimized conformation of **1** (SPARTAN, AMI force field) with one bound initiator molecule (**2**) in the cavity; (b) the monomers used in this study; (c) a representation of the ATRP process.

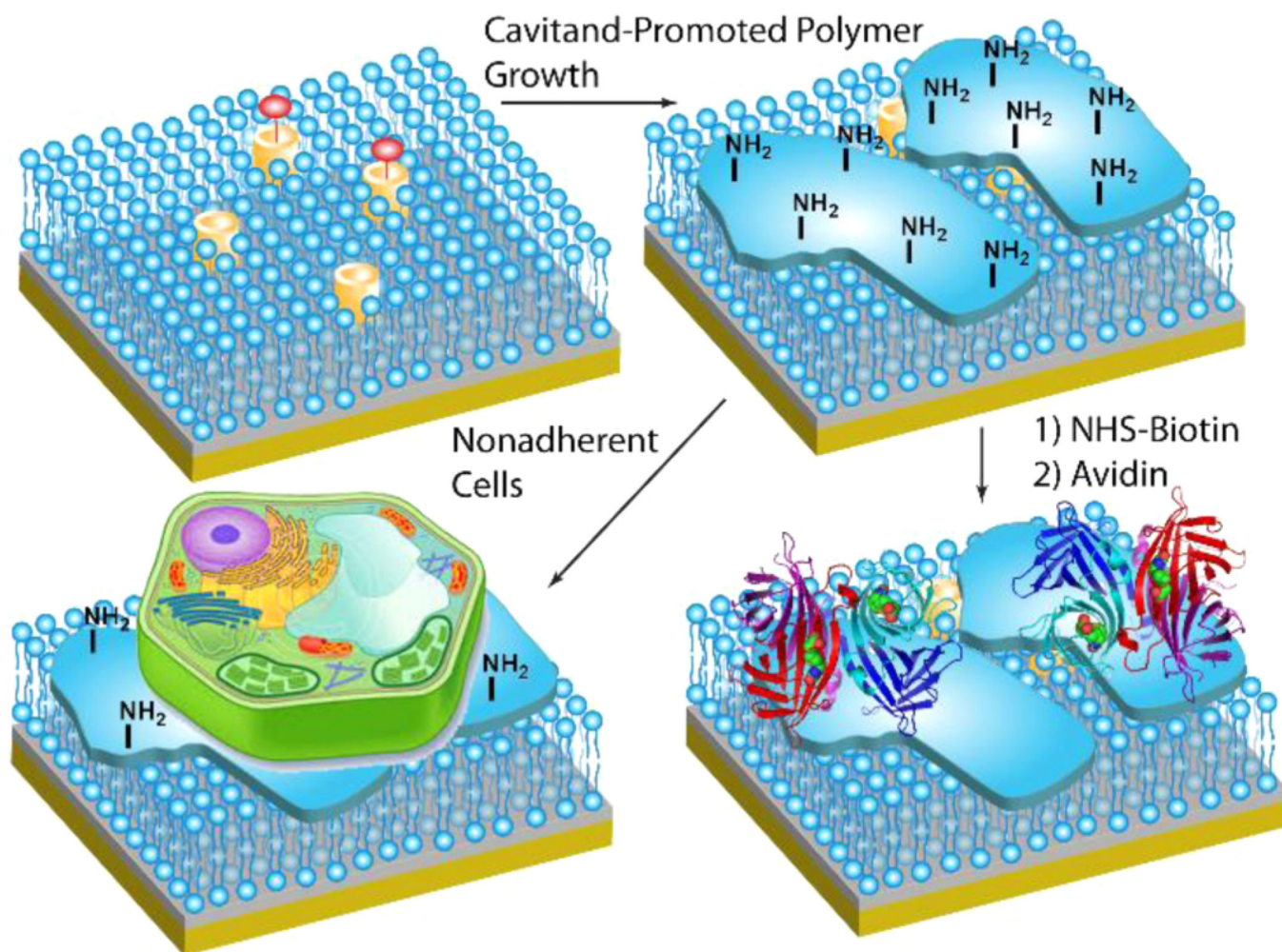


Figure 2.
In situ functionalized polymer growth at a bilayer interface and application to protein and cell adhesion.

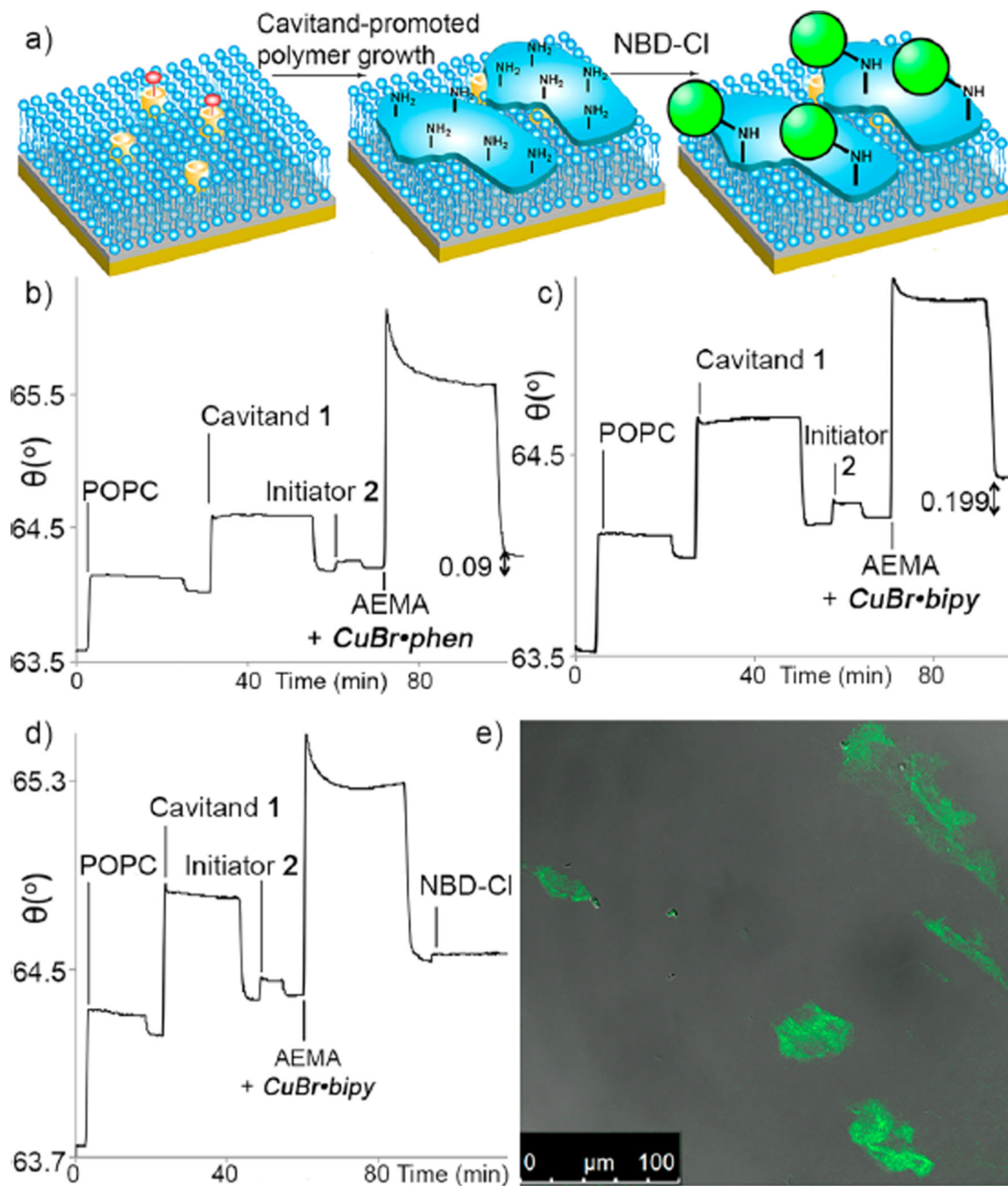


Figure 3.

(a) Cavitand-mediated aminopolymer growth and reactivity at a bilayer interface; (b,c) SPR sensorgrams of the process with different catalysts; (d) SPR sensorgram of the reaction with NBD-Cl; (e) confocal microscopy image of the dyed polymer at the bilayer interface.

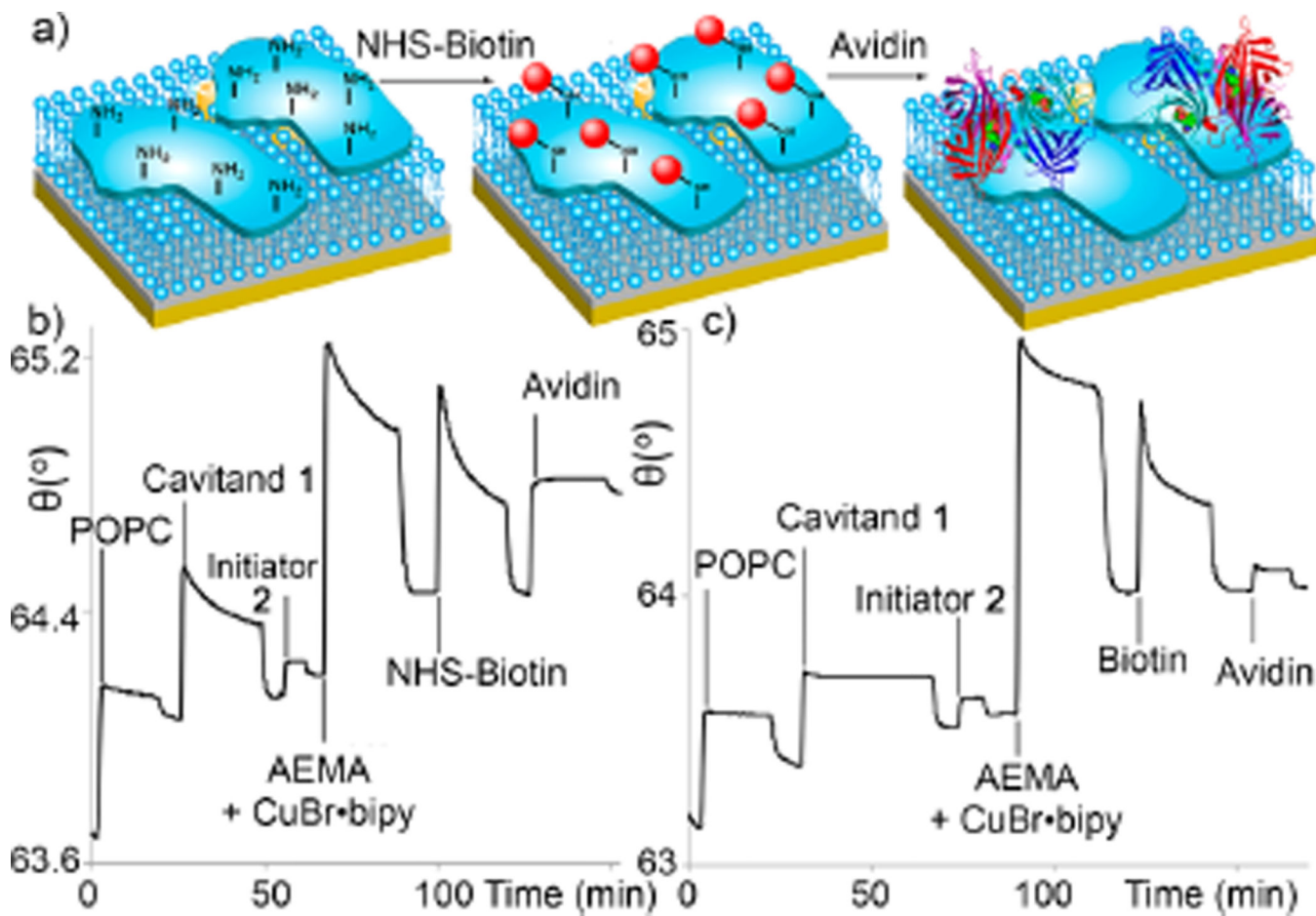


Figure 4. (a) Surface polymer derivatization and protein recognition; SPR sensorgrams of (b) covalently biotinylated poly(AEMA) recognizing avidin in situ and (c) control experiment with unactivated biotin.

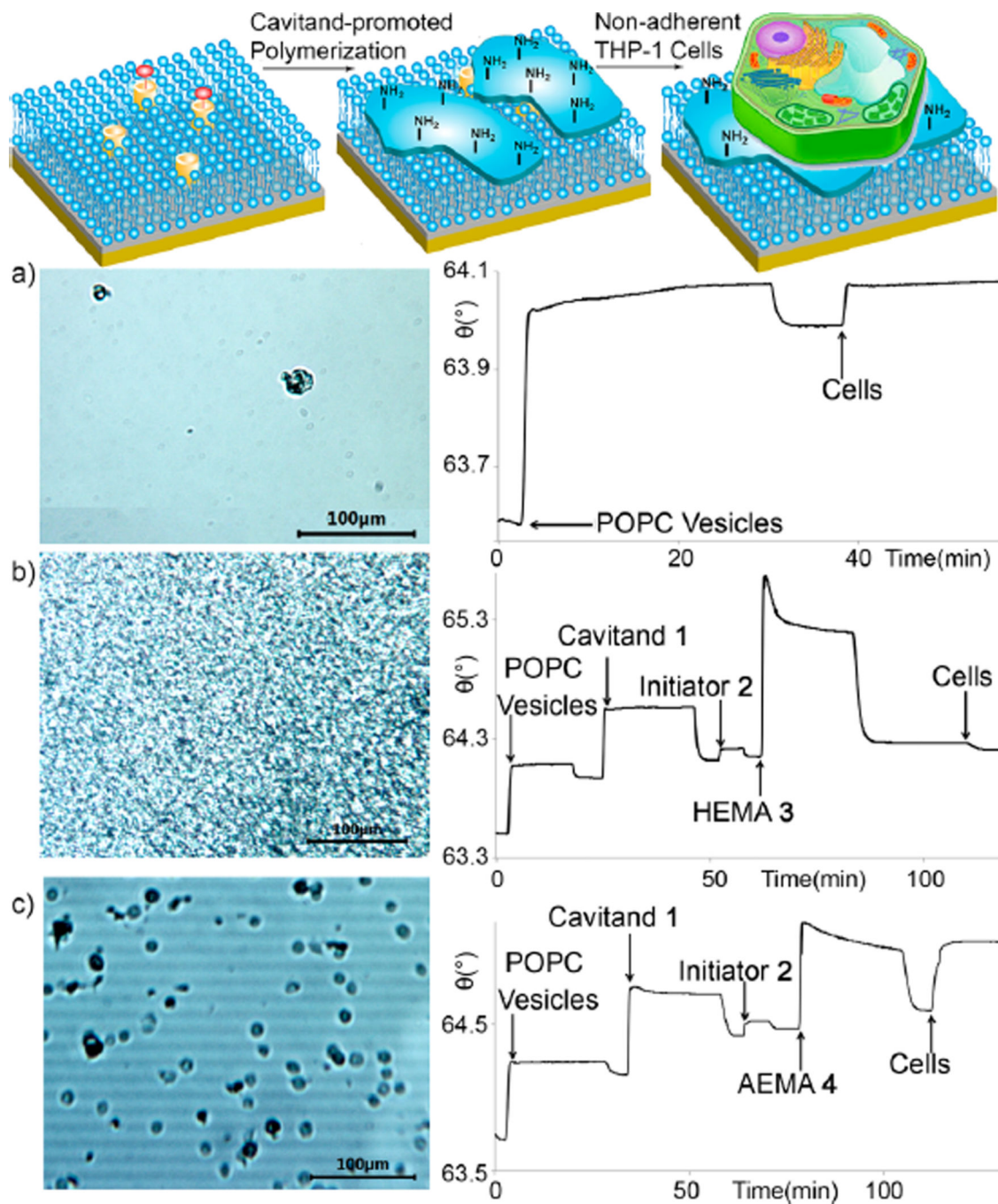


Figure 5. Nonadherent cell immobilization at the polymer surface; microscope image and SPR sensorgrams of cell recognition at (a) pristine POPC bilayer, (b) poly(HEMA)-coated POPC:1:2 interface, and (c) cationic poly(AEMA)-coated POPC:1:B interface.